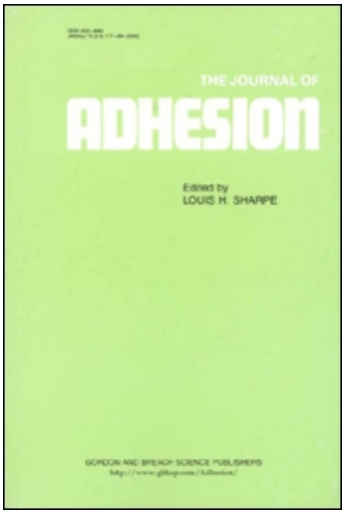


## The Journal of Adhesion

Publication details, including instructions for authors and subscription information:
http://www.informaworld.com/smpp/title~content=t713453635

# Numerical Analysis of the Constrained Blister Test

Yeh-Hung Lai[a]; David A. Dillard[a]
[a] Engineering Science and Mechanics Department, Virginia Polytechnic Institute and State University, Blacksburg, Virginia, U.S.A.

**To cite this Article** Lai, Yeh-Hung and Dillard, David A.(1990) 'Numerical Analysis of the Constrained Blister Test', The Journal of Adhesion, 33: 1, 63 — 74
**To link to this Article: DOI:** 10.1080/00218469008030417
**URL:** http://dx.doi.org/10.1080/00218469008030417

*J. Adhesion*, 1990, Vol. 33, pp. 63–74
Reprints available directly from the publisher
Photocopying permitted by license only

Printed in the United Kingdom

# Numerical Analysis of the Constrained Blister Test†

YEH-HUNG LAI and DAVID A. DILLARD‡

*Engineering Science and Mechanics Department, Virginia Polytechnic Institute and State University, Blacksburg, Virginia 24061-0219, U.S.A.*

*(Received March 30, 1988; in final form August 1, 1990)*

The constrained blister test is investigated through finite element analysis to determine the applicabilities and the limitations of the new technique. Numerical results confirm that the strain energy release rate asymptotically approaches a constant value. These results also show that the test technique and the approximate solution for strain energy release rate are applicable for some practical cases.

KEY WORDS Adhesive; fracture test; constrained blister test; blister test; finite element analysis; strain energy release rate.



## INTRODUCTION

Over the years, a large number of test geometries have been devised for evaluating the properties of *in situ* adhesives. The use of fracture mechanics has provided a rational basis for the design of structural components and a number of tests have been developed for measuring these properties. These include such tests as the double cantilever beam (DCB) test originally developed by Mostovoy,[1] the cone pull-out test developed by Anderson *et al.*,[2] and the blister test originally employed for paints by Dannenberg,[3] and later adapted to structural adhesives by Williams.[4] Each of these tests has certain advantages and disadvantages and each may be modified to provide some degree of mixture between mode I, II and III crack growth. Among these tests, the axisymmetric blister specimen offers an attractive alternative for environmental exposure because the diffusion occurs nearly perpendicular to the debond so that penetration from the sides does not present a problem.[5] Also, because of the axisymmetric nature of the blister specimen, the non-uniformity of the stress field along the debond front is much less than for a finite width specimen. One of the

† Presented at ehe Eleventh Annual Meeting of The Adhesion Society, Inc., Charleston, South Carolina, U.S.A., February 21–24, 1988.
‡ Corresponding author.

most difficult problems associated with the blister specimen is the determination of the debond radius. Although several techniques have been proposed to identify the increments of crack growth and to detect debond initiation,[6,7] adequate information about actual debond size is still quite difficult to obtain.

Measurement of the debond size is important for two reasons—the determination of the increments in crack growth and the evaluation of the debond radius for calculation of the strain energy release rate. Anderson *et al.*[7] discuss closed form and numerical solutions for the strain energy release rate and have identified regions of applicability for formulae for a penny-shaped crack between two semi-infinite media and for plate theory. For the simplest case where thin plate assumptions with small deformations are applicable, the closed form solution is:

$$G = \frac{3(1-\nu^2)}{32Et^3} p^2 a^4 \tag{1}$$

where $G$ is the strain energy release rate, $\nu$ is the Poisson's ratio, $E$ is the Young's modulus, $p$ is the pressure in the blister, $a$ is the debond radius, and $t$ is the thickness of the specimen.

Since radius appears to the fourth power, small errors in measuring the debond will result in significant errors in estimating $G$. On the other hand, in the case of a relatively thin specimen with the membrane effect involved, the above solution is not applicable. For this case, Gent and Lewandowski[8] proposed a solution for strain energy release rate with the form: $G = 0.65py$, where $y$ is the deflection of the center of the blister, which is proportional to the cube root of pressure and is also a function of debond radius. Recently, Allen and Senturia proposed models for the case of thin films in the blister test of annular and rectangular shape with and without residual stresses.[9,10] This "island" blister geometry has also been extended to a constant strain energy release rate "peninsula" blister geometry while retaining the high strain energy release rate nature of the island blister.[11,12]

More recently, a modification of the blister test called the constrained blister test which permits nearly constant strain energy release rate testing of adhesive bonds was proposed independently by Dillard *et al.*[13,14] and Moet *et al.*[15] By placing a flat constraint above the blister to limit its deformation (Figure 1), the volume displaced is approximately proportional to the debond area. Under constant pressure loading, this results in a nearly constant strain energy release rate test. The energy released as the debond grows may be expressed as:

$$G\,\delta A = p\,\delta V - \delta U - \delta Z \tag{2}$$

where $\delta A$ is the variation of the debond area, $\delta V$ is the variation in displaced volume, $\delta U$ is the variation of the strain energy, and $\delta Z$ is the variation of the dissipated energy due to bulk viscoelastic and frictional effects.

If one may neglect the energy dissipation due to viscoelastic effects and frictional slipping, and if the change in strain energy as the blister grows is negligible, the strain energy release rate is given by:

$$G = phq \tag{3a}$$

where $h$ is the constraint height, and $q$ is the correction factor.

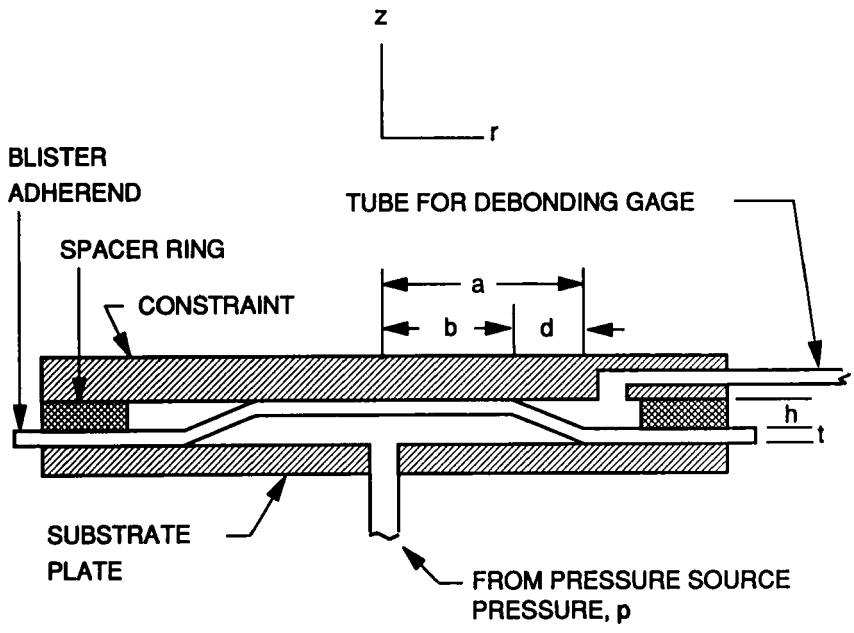


FIGURE 1 Constrained blister test geometry.

For our purposes, it is understood that $G$ represents the total energy dissipated in the vicinity of the crack tip, and hence includes the thermodynamic work of adhesion plus near-field viscous/plastic dissipation. If no viscous behavior is present, the critical value of $G$ is a single value at which failure occurs and below which debonding does not occur. If viscous mechanisms are present, $G_{cr}$ is a function of the debond rate.[7] If the suspended region of the blister may be approximated as a linear shape the correction factor becomes:

$$q = \left(1 - \frac{d}{2a}\right) + \left(\frac{d}{3a} - \frac{1}{2}\right)\frac{\partial d}{\partial a} \tag{3b}$$

where $d$ is the length of the suspended region.

A series of preliminary tests on adhesive tapes showed the existence of a state of nearly constant $G$ and suggested the applicability of the constrained blister test for environmental exposure research.[14] In this paper, more cases are examined to verify the applicability of Eq. (3) by using the numerical technique described in the following section. The necessary assumptions will be shown to be reasonably accurate for many practical geometries.

## FINITE ELEMENT ANALYSIS

In order to model the contact between the blister and the upper constraint, the finite element program called ABAQUS (version 4-7) was used because of its

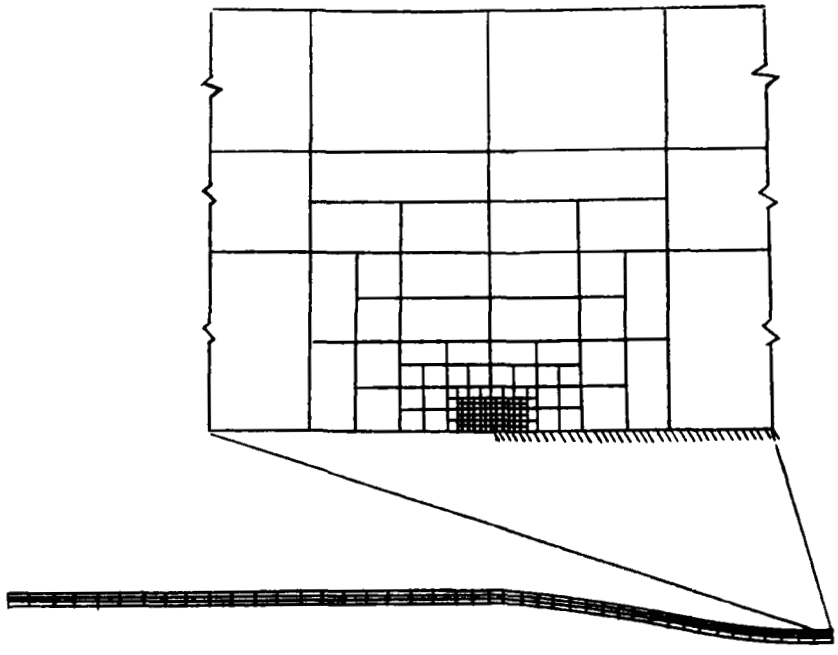

FIGURE 2 Typical deformed mesh of the finite element model for an aluminum specimen.



capabilities to handle contact problems. Since the geometry and boundary conditions are axisymmetric, an axisymmetric, biquadratic element was used. All the materials analyzed were assumed to be linearly elastic. Thus, although the fracture process may involve considerable localized viscoelastic/plastic dissipation, gross viscoelastic/plastic effects away from the fracture zone are not considered. ABAQUS has been used to analyze several adhesive systems and geometric configurations. Only two cases are reported herein: 1) an aluminum blister and 2) a tape blister for a polyester backing. One of the typical deformed meshes and the refined mesh near the crack front of an aluminum specimen are shown in Figure 2.

## RESULTS AND DISCUSSIONS

In order to verify the applicability of Eq. (3) for the constrained blister test, typical cases were analyzed with different parameters. Figures 3–7 are the cases for aluminum 6061-T6 specimens which have a Young's modulus of 68,930 MPa and Poisson's ratio of 0.3. Figures 8–10 are the cases for adhesive tapes with polyester backing. In these cases, a Young's modulus of 750 MPa and Poisson's ratio of 0.36 was used. Figure 3 illustrates a typical stress distribution obtained by a geometrically nonlinear analysis at the lower side of an aluminum specimen which has a thickness of 3 mm, a constraint height of 2 mm and is subjected to a

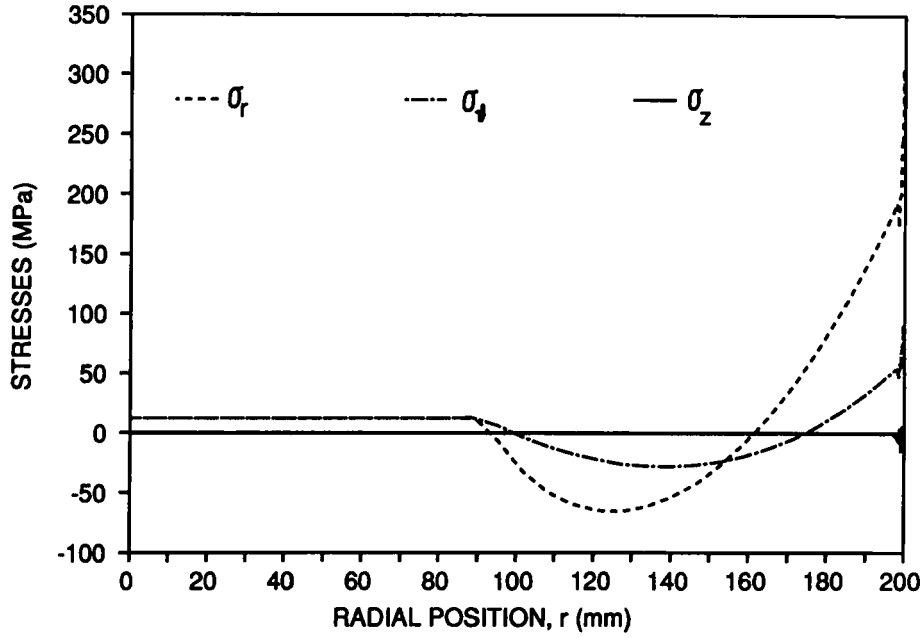


FIGURE 3 Stress distribution along the lower surface of an aluminum specimen using the geometrically nonlinear analysis.

pressure of 200 kPa. The legends denoted "$\sigma_r$", "$\sigma_\theta$" and "$\sigma_z$" stand for the stresses in the radial, circumferential, and axial directions, respectively. This convention will be used throughout the following figures. Starting from $r = 0$, a uniform stress distribution is seen in the area that contacts the upper constraint. In the suspended region, $\sigma_r$ and $\sigma_\theta$ change signs twice because of the sigmoidal bending and, finally, the stresses begin to grow rapidly or oscillate as one approaches the singular crack tip region at $r = 200$ mm. Away from the crack front, the stress in the $z$ direction, which has the same magnitude as the applied pressure, is very small compared with the other two stress components so that it is hardly visible in the figure.

Figure 4 illustrates a typical stress distribution obtained by nonlinear analysis at the mid-plane of the same aluminum specimen as in Figure 3. It is seen that membrane stretching stresses, $\sigma_r$ and $\sigma_\theta$, obtained from the nonlinear analysis, remain at the same magnitude within the contacted region but split and decrease beyond $r = b$. The small drop of $\sigma_z$ at the inner end of the suspended region indicates the effect of the compressive reaction force from the upper constraint in this local region.

Figure 5 shows the deformed profiles of the aluminum specimen obtained from the nonlinear analyses. It should be noted that the $z$-axis is greatly enlarged. It is seen that the suspended region is not a straight line. Since the correction fact, $q$, is based on the assumption of a linear suspended region, this nonlinearity could induce error when calculating the strain energy release rate from Eq. (3).

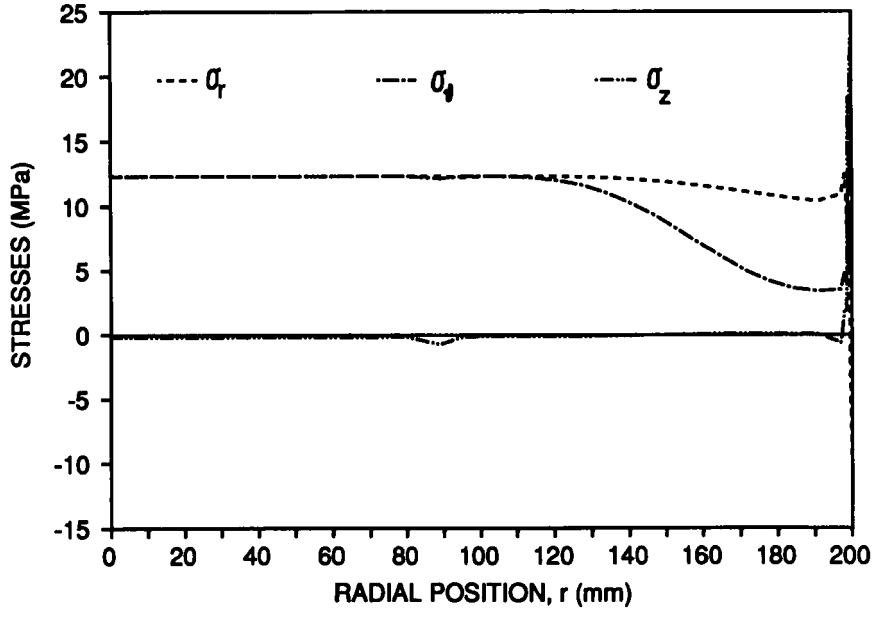


FIGURE 4 Stress distributions of an aluminum specimen at the mid-plane for geometrically nonlinear analysis.

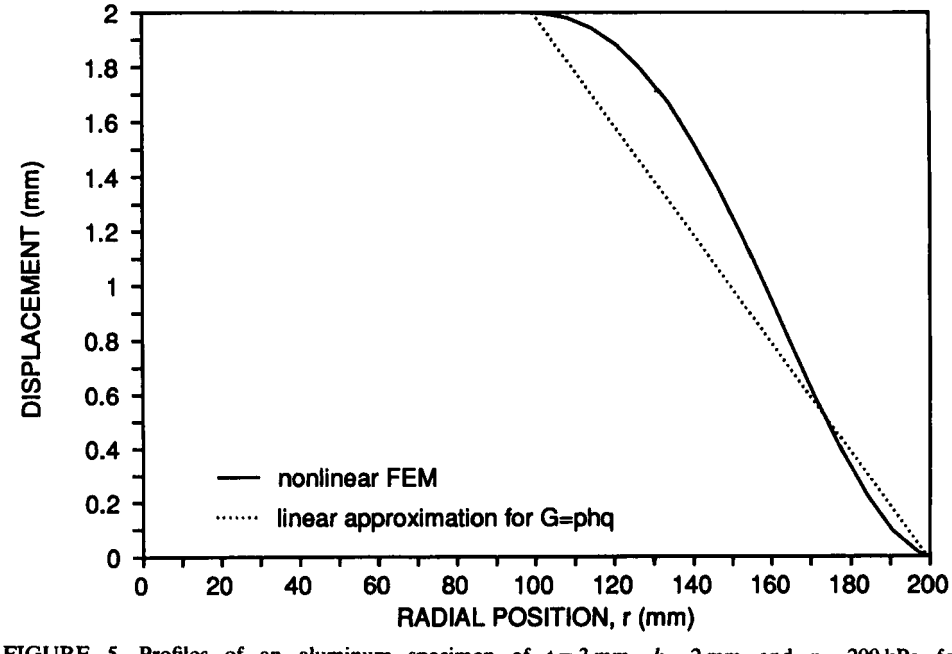


FIGURE 5 Profiles of an aluminum specimen of $t = 3$ mm, $h = 2$ mm and $p = 200$ kPa for geometrically nonlinear analysis and linear approximation.

However, by examining the difference of the volume, the error of strain energy release rate due to this approximation is about 0.5%.

Figures 6–10 give strain energy release information for both the aluminum and adhesive tape cases. The legend denoted "$G = phq$" represents the strain energy release rates which are evaluated from Eq. (3). It is noted that when calculating $q$ using Eq. (3b), the length of suspended region, $d$, is not calculated from analytical expressions, but from the finite element results. It is assumed that similar values for $d$ would have been observed experimentally; furthermore, small errors in $d$ do not significantly affect the values of strain energy release rate. The legends, "$J$-INT (FEM)" stands for the $J$-integral curves which are obtained from the finite element analysis. The legend "$G = ph$" stands for the strain energy release rate in the limiting case when $q = 1$, which corresponds to $d/a = 0$. This approximation is seen to be substantially in error for most cases considered.

Figure 6 illustrates the strain energy release rates *versus* debond radius for the case of an aluminum specimen which has the same dimensions and material properties as those in the previous figures. Good agreement for total strain energy release rate is seen between the analytical solution and the FEM results. The gap between the curves denoted "$G = phq$" shows the necessity for the correction factor, $q$. It should be noted that $q$ is obtained from Eq. (3b) by neglecting $\partial d/\partial a$. Justification of this assumption is based on experimental observations[14] and is also demonstrated numerically in the following section.

One concern in developing Eq. (3) and Eq. (2) was whether the blister region



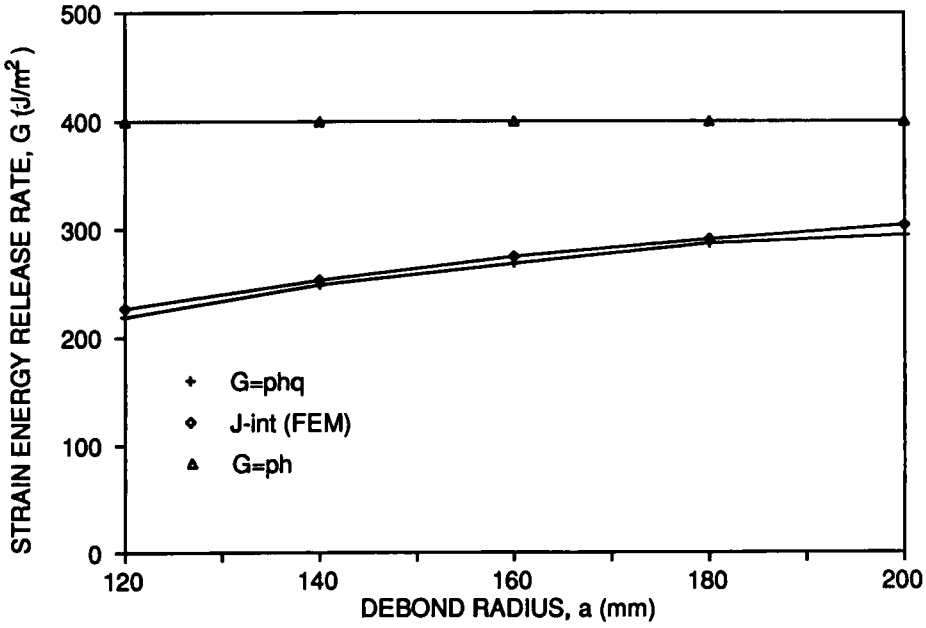


FIGURE 6 Strain energy release rate *versus* debond radius for an aluminum specimen of $t = 3$ mm, $h = 2$ mm and $p = 2$ kPa.

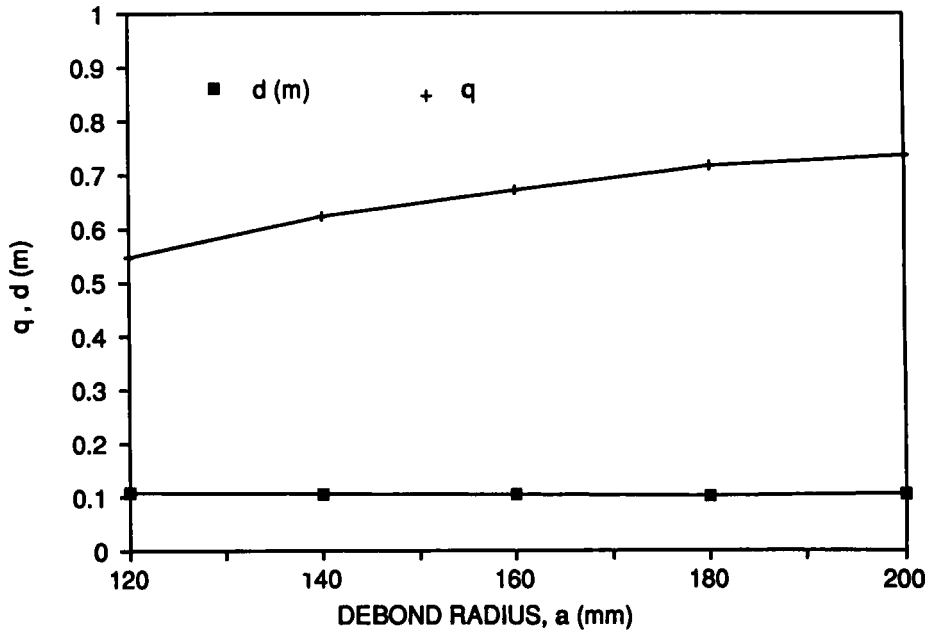


FIGURE 7 Correction factor and the length of suspended region *versus* debond radius for an aluminum specimen of $t = 3$ mm, $h = 2$ mm and $p = 200$ kPa.



in contact with the constraint would slip as the blister grows, thereby dissipating a portion of the input work. By changing coefficients of friction from 0.0 to 1.0 for the ABAQUS contact elements, it is found that only a negligible change ($< 0.01\%$) in the strain energy release rate occurs, which shows that neglecting the frictional dissipation is reasonable in deriving Eq. (3).

Figure 7 shows the effect of the debond radius on the correction factor and the length of the suspended region. It shows that $d$ remains nearly constant as $a$ increases. Therefore, the assumption of neglecting $\partial d/\partial a$ is reasonable and $q$ is primarily influenced by $a$ only. It is seen that $q$ is smaller than 0.75, thus, the error between the equations, $G = ph$ and $G = phq$, would be greater than 25% and it is important to determine $q$. However, it should be noted that since $a$ and $d$ are to the first order in Eq. (3b), the error of $q$ and, consequently, error of $G$, resulting from a measuring error in $a$ or $d$ would be quite small. In the analysis of the aluminum specimens, the total strain energy release rates considered were in the range of 210–320 J/m$^2$ and the maximum principal stress does not exceed 275 MPa, a typical aluminum yielding stress, except very near the singular point (the size of plastic zone is about 0.05% of the thickness). It should be noted that for an adhesive system with an adhesive fracture energy higher than 320 J/m$^2$, one can either increase pressure or increase constraint height to study debond. It should be noted, however, that higher pressure or constraint height could induce yielding in the blister adherend and thus, induce a large error for the strain energy release rate. In the analysis of this aluminum specimen case, it is also seen

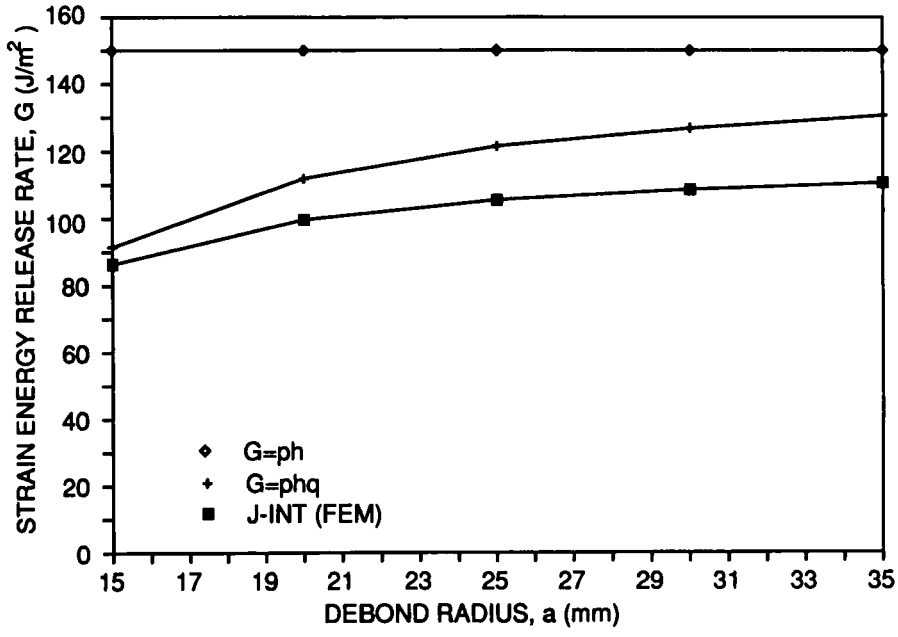


FIGURE 8 Strain energy release rate *versus* debond radius for an adhesive tape specimen of $t = 0.3$ mm, $h = 1.5$ mm and $p = 100$ kPa.



that for a small debond radius ($a < 120$ mm), the specimen would not touch the upper constraint. This indicates that one usually needs large specimens and equipment to perform the test on aluminum adherends. Special reinforcement of the constraint may be required to minimize its deflection.

Figure 8 illustrates the relationship between the energy release rates and debond radius for the tape specimen with an $h$ of 1.5 mm and $t$ of 0.3 mm, corresponding to three layers of adhesive tape in the previous tests.[13,14] The applied pressure is 100 kPa. Although the percentage difference between the FEM analysis and the Eq. 3a is between 8 and 13 percent in this figure, it is seen that for the FEM analysis and for the approximate equation (Eq. 3a), the strain energy release rates increase as debond radius increases. For both approaches, the slopes of both curves decrease as debond radius increases. It is seen that if the debond radius is large enough, the test would become a nearly constant strain release rate test.

From Figures 6, 7, and 8, it is seen that as $a$ becomes larger, the gradient of $q$, and thus the rate of increase in $G$ with respect to $a$, becomes smaller. Since $q$ and $h$ are held constant if $a$ is large enough, energy release rates would be nearly constant; *i.e.*, the test would be a nearly constant strain energy release rate test. The magnitude of the correction factor, however, may not be negligible.

Figure 9 illustrates the strain energy release rate *versus* pressure for the tape case. The percentage difference between FEM analysis and the Eq. 3a increases from 9% to 20% as pressure increase from 80 kPa to 350 kPa. Approximate

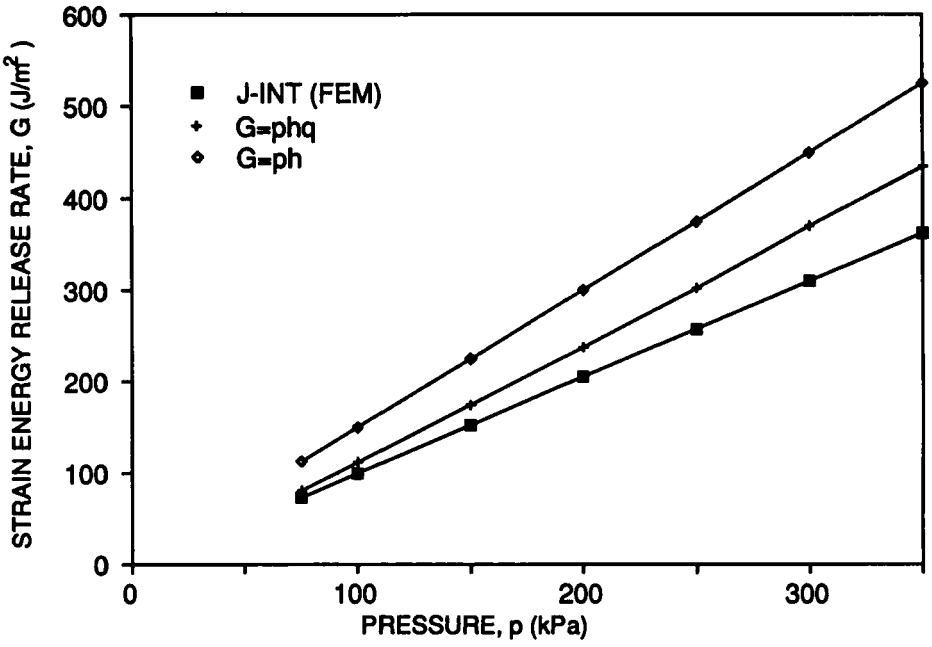


FIGURE 9 Strain energy release rate *versus* pressure for an adhesive tape specimen of $t = 0.3$ mm, $h = 1.5$ mm and $a = 20$ mm.

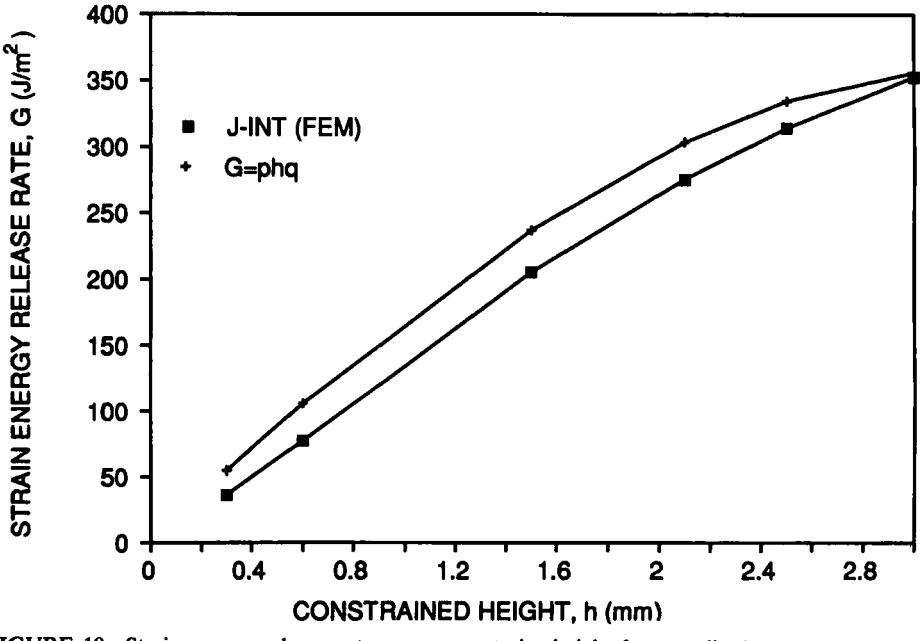


FIGURE 10 Strain energy release rate *versus* constraint height for an adhesive tape specimen of $t = 0.3$ mm, $a = 20$ mm and $p = 200$ kPa.

linearity is seen between $G$ and $p$. Figures 8, 9 and 10 all indicate that there is greater deviation between Eq. 3a and the finite element results for the membrane-like tape case than for the case of a plate-like aluminum adherend. The tape case required a geometrically nonlinear analysis because of the large deformation, and convergence was more difficult to obtain. It is possible that more energy is being stored in the membrane than in the plate, thereby reducing the energy available for debond propagation. We cannot explain the larger differences, but suggest that further analysis is necessary to understand the process better.

Figure 10 illustrates the strain energy release rate *versus* constraint height. It should be noted that if $h$ is larger than 3 mm, the specimen does not touch the upper constraint. It is seen that $G$ increases as $h$ increases; however, the percentage difference between those two analyses decreases as $h$ increases. An approximate linearity is also seen for the relation of $G$ and $h$.

## CONCLUSIONS

A series of finite element analysis were performed to verify the applicability of a simple approximate solution for the constrained blister test, a technique offering a state of nearly constant strain energy release rate. Two materials, aluminum and adhesive tape, which were chosen to represent relatively stiff and relatively soft cases, have been investigated. For the aluminum case, which is basically a plate problem, the numerical analysis and the approximate solution are in good agreement. Larger deviation between the numerical and approximate solution for the tape specimen, which is basically a membrane problem, was observed. The results from these two specimens indicate that the approximate solution is not applicable for every material and geometry. Although the numerical analysis does show possible problems with the approximate solution for membrane cases, it does verify that the constrained blister test is a nearly constant strain energy release rate geometry. The numerical solutions also verify that the strain energy release rate does increase nearly linearly with pressure and constraint height, and that the correction factor $q$ is necessary to estimate the release rate accurately.



### Acknowledgements

The authors would like to acknowledge the financial support of Texas Research Institute, Inc. (Dr. J. S. Thronton), the Virginia Center for Innovative Technology (Dr. C. Spencer), and the Office of Naval Research (Dr. L. Peebles). We are also grateful to Yeou Shin Chang for his helpful comments.

### References

1. S. Mostovoy and E. J. Ripling, Final Report, Contract No. N00019-74-c-0274. Mater. Lab., Glenwood, Illinois, U.S.A. 1975.
2. G. P. Anderson, K. L. DeVries and M. L. Williams, *Int. J. Fract.* **10,** 565–583 (1974).
3. H. Dannenberg, *J. Appl. Polym. Sci.* **5,** 125–134 (1961).

4. M. L. Williams, *J. Appl. Polym. Sci.* **13,** 29–40 (1969).
5. D. R. Lefebvre, D. A. Dillard and H. F. Brinson, *Experimental Mechanics* **28,** 38–44 (1988).
6. W. B. Jones, Ph.D. Dissertation, Univ. of Utah, Salt Lake City, 1970.
7. G. P. Anderson, S. J. Bennett and K. L. DeVries, *Analysis and Testing of Adhesive Bonds* (Academic Press, New York, 1977).
8. A. N. Gent, L. H. Lewandowski, *J. Appl. Polym. Sci.* **33,** 1567–1577 (1987).
9. M. G. Allen and S. D. Senturia *Preprints Am. Chem. Soc. Div. of Polymeric Materials: Science and Engineering* **56,** 735–739 (1987).
10. M. G. Allen and S. D. Senturia, *J. Adhesion* **25,** 305–314 (1988).
11. D. A. Dillard, Y. H. Lai, Y. S. Chang, T. Corson, Y. Bao, *Proc. 1990 SEM Conference on Experimental Mechanics,* Albuquerque, NM, U.S.A. 1990, pp. 575–582.
12. D. A. Dillard and Y. Bao, *J. Adhesion*, in review.
13. D. A. Dillard and Y. S. Chang, VPI Report, VPI-E-87-24, Blacksburg, Virginia, Sept. 1987.
14. Y. S. Chang, Y. H. Lai and D. A. Dillard, *J. Adhesion* **27,** 197–211 (1989).
15. M. J. Napolitano, A. Chudnovsky, A. Moet, *Preprints Am. Chem. Soc. Div. Polymeric Materials: Science and Engineering* **56,** 755–759 (1987).